ACS APPLIED MATERIALS & INTERFACES

Research Article

www.acsami.org

New Fluorescent Metal-Ion Detection Using a Paper-Based Sensor Strip Containing Tethered Rhodamine Carbon Nanodots

Yujun Kim, Geunseok Jang, and Taek Seung Lee*

Organic and Optoelectronic Materials Laboratory, Department of Advanced Organic Materials and Textile System Engineering, Chungnam National University, Daejeon 305-764, Korea

Supporting Information

ABSTRACT: A strip of tethered rhodamine carbon nanodots (C-dots) was designed for selective detection of Al^{3+} ion using a Förster resonance energy transfer (FRET)-based ratiometric sensing mechanism. The probe consisted of rhodamine B moieties immobilized on the surface of water-soluble C-dots. Upon exposure to Al^{3+}, the rhodamine moieties showed a much enhanced emission intensity via energy transfer from the C-dots under excitation at their absorption wavelength. The detection mechanism was related to the Al^{3+}-induced ring-opening of rhodamine on C-dots through the chelation of the rhodamine 6G moiety with Al^{3+}, leading to a spectral overlap of the absorption of C-dots (donor) and the emission of ring-opened rhodamine (acceptor). In addition, a paper-based sensor strip containing the tethered rhodamine C-dots was prepared for practical, versatile applications of Al^{3+} sensing. The paper-based sensor could detect Al^{3+} over other metal ions efficiently, even from a mixture of metal ions, with increased emission intensity at long-wavelength emission via FRET. Sensing based on FRET of C-dots is color-tunable, can be recognized with a naked eye, and may provide a new platform for specific metal-ion sensing.

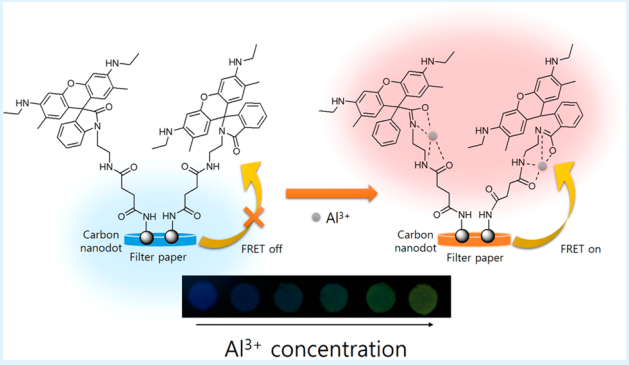

KEYWORDS: *carbon dots, rhodamine 6G, FRET, aluminum sensing, paper-based sensor strip*

INTRODUCTION

The recently discovered carbon nanodots (C-dots) represent a fascinating class of carbonaceous and fluorescent nanomaterials consisting of a discrete quasispherical shape with sizes below 10 nm.[1,2] C-dots present a number of advantages over other fluorescent materials in their high solubility in water, high chemical resistance, easy functionalization, high resistance to photobleaching, low toxicity, and good biocompatibility.[1−6] C-dots can be prepared by various synthesis routes including arc discharge, combustion, hydrothermal preparation, microwave pyrolysis, laser ablation, and plasma treatment.[1,2,7−12] Accordingly, the fabrication of C-dots is not source-limited, that is, C-dots can be prepared from a wide variety of materials, such as small organic molecules,[13,14] egg,[15] carbohydrate,[16] and silk,[17] that have been explored in versatile applications such as bioimaging,[18,19] chemosensors,[20−22] temperature sensors,[23] drug carriers,[24,25] photocatalysts,[26] and photothermal therapy.[27] Although this new category of nanomaterials is considered to be a potential candidate to substitute for quantum dots, some of the shortcomings should be eliminated, for instance, their inability to emit strong long-wavelength fluorescence and to dissolve in organic solvents other than water.[28,29]

Förster resonance energy transfer (FRET)-based ratiometric probes involve the observation of target-triggered ratiometric changes in the fluorescence intensity at two different wavelengths, which could provide correction for eliminating environmental effects, leading to minimization of any possible noise and increase in the dynamic response.[30−33] Rhodamine derivatives have been proven an efficient acceptor and are thereby used as FRET-based ratiometric probes for various metal ions.[34−37] Rhodamine derivatives with a spirolactam (closed) form are colorless and nonfluorescent, whereas those with an open-ring amide form induced by suitable metal ions give rise to a pink color appearing with strong fluorescence.[38−40]

Monitoring metal ions is critical in the fields of environmental protection and human health. Among many metal ions, the Al^{3+} ion has been proven to have many detrimental effects on the human body, including neurotoxicity, Parkinson's disease, Alzheimer's disease, and cancer.[41,42] Therefore, a variety of sensing techniques were developed for this ion during the past decades, including spectrofluorometry,[43−46] atomic absorption spectroscopy,[47,48] and voltammetry.[49−51] Although numerous Al^{3+} sensors have been developed so far, the design of structurally simple and efficient devices for improving the sensitivity of solid-state detection still remains challenging. Moreover, among such detection methods, fluorescent probes for Al^{3+} based on FRET have been rarely developed because of the complicated architecture of energy donor and acceptor.

Received: May 30, 2015
Accepted: June 26, 2015
Published: June 26, 2015

DOI: 10.1021/acsami.5b04724
ACS Appl. Mater. Interfaces 2015, 7, 15649−15657

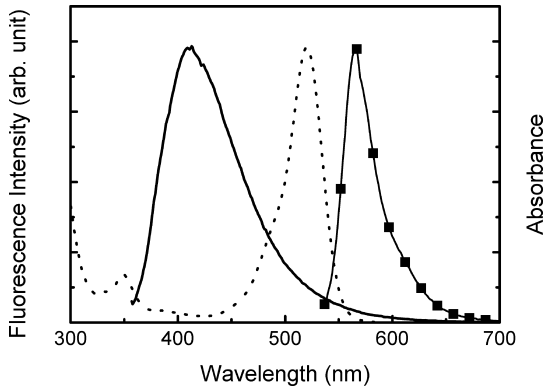

Figure 1. Spectroscopic overlap between emission of C-dots in aqueous solution (solid line, excitation wavelength λ_{ex} = 350 nm) and absorption (dotted line) and emission spectra (■, excitation wavelength λ_{ex} = 526 nm) of R6G (lactam ring opened by acid treatment) in ethanol solution.

Scheme 1. Synthesis of C-dots-R6G

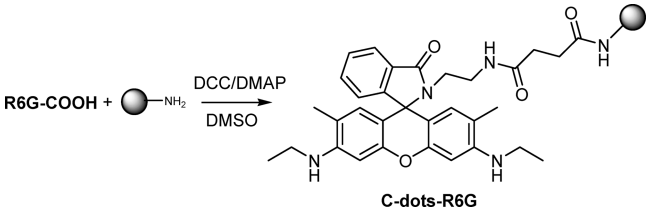

Inspired by the outstanding features of C-dots, we propose using C-dots as an energy donor and the rhodamine moiety as an energy acceptor for the modulation of FRET to detect Al^{3+}. In FRET-related applications, covalent coupling is used for the immobilization of rhodamine on the surface of C-dots for specific recognition. To our knowledge, FRET-based detection mechanisms using C-dots have been rarely reported.[52] Similar to our work, a C-dots-based sensor for Hg^{2+} has been recently reported.[53] However, Lan et al. reported that the mercury ion quenched the C-dots while preserving the initial fluorescence of rhodamine, in which case FRET did not occur. Until now, most of the sensing protocols based on fluorescent materials have been demonstrated mainly in their solution, which limits their practical usefulness. The main advantages of solid sensors over solution sensors are the easy handling and facile incorporation into devices.[54−56] In this work, a paper-based sensor strip containing the C-dots conjugated with a rhodamine moiety was prepared to demonstrate the practical application of C-dots in the detection of metal ions. Here, FRET was exploited on the paper upon exposure to Al^{3+}. This will be more practical for Al^{3+} detection than a solution-based system because of the use of commercial filter paper with its availability and convenience. This is a promising sensor platform to achieve a paper-based sensor in a practical application.

EXPERIMENTAL METHODS

Materials. Acrylic acid, dichloromethane, dimethyl sulfoxide (DMSO), and ethanol were purchased from Samchun (Korea). 1,2-Ethylenediamine, rhodamine 6G (R6G), succinic acid, *N*,*N*-dimethylformamide (DMF), *N*-(3-(dimethylamino)propyl)-*N*′-ethylcarbodiimide hydrochloride (EDC), *N*-hydroxysuccinimide (NHS), *N*,*N*′-dicyclohexylcarbodiimide (DCC), and 4-(dimethylamino)-pyridine (DMAP) were purchased from Sigma-Aldrich and used as received. Metal-ion solutions of Cd^{2+}, Cu^{2+}, Fe^{3+}, Fe^{2+}, Mg^{2+}, Ni^{2+}, Al^{3+}, and Zn^{2+} were prepared from their perchlorate salts; a solution of Hg^{2+} was prepared from its cyanide salt. Standard stock solutions of all ions were prepared using deionized water or ethanol. Dialysis membranes (MWCO of 13 000) were purchased from Aldrich.

Synthesis of C-dots. Acrylic acid (5.49 g, 80.0 mmol) and 1,2-ethylenediamine (5.35 mL, 80.0 mmol) were dissolved in deionized water (20 mL). Next, the transparent solution was put into a microwave oven (700 W) and heated for 7 min. After cooling to room temperature, water (20 mL) was added to the mixture to dissolve the synthesized C-dots. The obtained yellowish solution was filtered through a cellulose acetate syringe filter (pore size of 0.2 μm) and

Scheme 2. Schematic Illustration for the FRET-Based Detection Mechanism of the C-dots-R6G in Response to Al^{3+}[a]

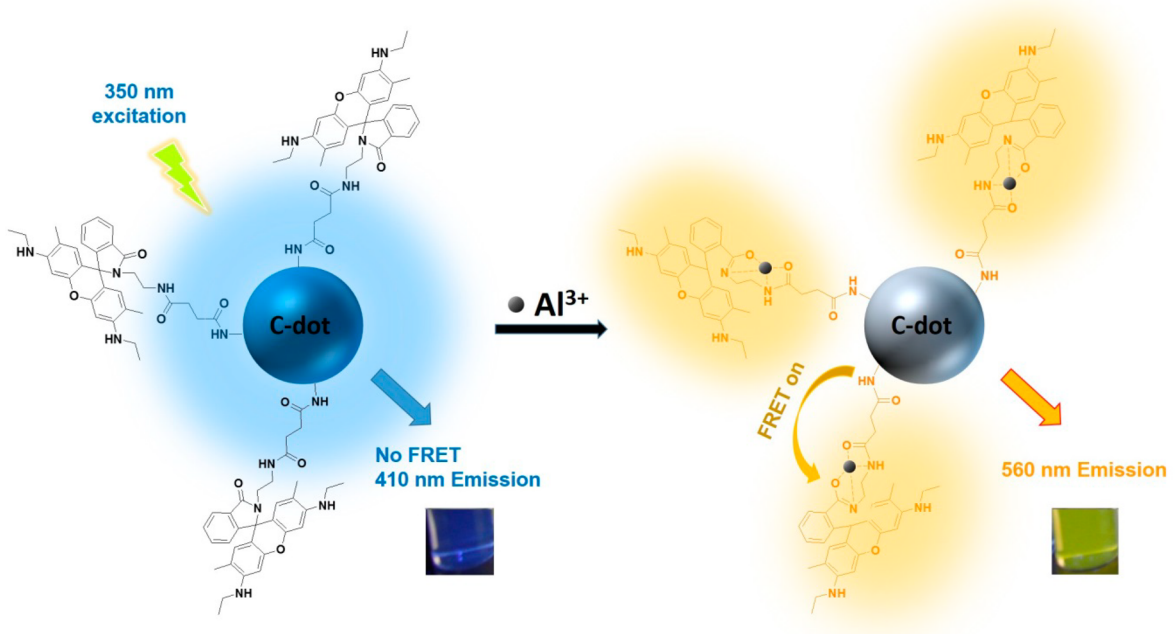

[a]Inset photographs were taken under UV illumination (365 nm).

DOI: 10.1021/acsami.5b04724
ACS Appl. Mater. Interfaces 2015, 7, 15649−15657

dialyzed against pure water through a dialysis membrane (MWCO of 13 000) for 48 h. Finally, C-dots were dried in a freeze-drying oven.

Synthesis of R6G-NH_2. R6G (4.80 g, 10 mmol) was dissolved in ethanol (60 mL). Next, 1,2-ethylenediamine (5 mL) was added dropwise with vigorous stirring at room temperature. After the addition, the mixture was heated to reflux with stirring for 12 h until the fluorescence of the solution disappeared. After the reaction, the mixture was cooled to room temperature, and the solvent was removed under reduced pressure. The resulting precipitates were collected by filtration and washed with cold ethanol three times (20 mL each). The crude product was purified by recrystallization from acetonitrile and dried under vacuum (3.02 g, yield 65%). ^{1}H NMR (300 MHz, $CDCl_3$) δ = 7.95 (dd, 1H), 7.47 (dd, 2H), 7.08 (dd, 1H), 6.36 (s, 2H), 6.25 (s, 2H), 3.53 (t, 2H), 3.23 (q, 4H), 2.37 (t, 2H), 1.92 (s, 6H), 1.34 ppm (t, 6H).

Synthesis of R6G-COOH. **R6G-NH_2** (200 mg, 0.4 mmol) and succinic acid (50 mg, 0.4 mmol) were dissolved in dry DMF in N_2 atmosphere. EDC (80 mg, 0.4 mmol) and NHS (50 mg, 0.4 mmol) were added to the reaction mixture and stirred at room temperature for 24 h. The solvent was removed under vacuum, then purified by silica-gel column chromatography (silica gel; ethanol/hexane as eluent) to afford **R6G-COOH** (112 mg, 46%). ^{1}H NMR (300 MHz, $CDCl_3$) δ = 7.95 (dd, 1H), 7.47 (dd, 2H), 7.08 (dd, 1H), 6.36 (s, 2H), 6.25 (s, 2H), 3.53 (t, 2H), 3.23 (q, 4H), 2.95 (t, 2H), 2.88 (t, 2H), 2.37 (t, 2H), 1.92 (s, 6H), 1.34 ppm (t, 6H).

Characterization. ^{1}H NMR spectra were recorded on a Bruker DRX-300 spectrometer with tetramethylsilane as the internal standard (Korea Basic Science Institute). UV−vis absorption spectra were taken with a PerkinElmer Lambda 35 spectrometer. Photoluminescence spectra were collected on a Varian Cary Eclipse equipped with a xenon lamp excitation source. IR spectra were recorded on a Bruker FT-IR spectrometer using KBr pellets (600−4000 cm^{-1}). Transmission electron microscopy (TEM) images were obtained on JEOL JEM-3010 operating at 200 kV accelerating voltage, using the images acquired with an ORIUS-SC 600 CCD camera (Gatan, Inc. Warrendale, PA). The sample for TEM was prepared by dropping a C-dots solution onto a 300 mesh copper grid coated with a carbon film. The X-ray photoelectron spectrum (XPS) of the sample was measured on a MultiLab 2000 XPS (Thermo VG Scientific). The zeta potentials of the C-dots were determined using a Malvern.

Synthesis of C-dots-R6G. C-dots (10 mg) and **R6G-COOH** (10 mg, 0.018 mmol) were dissolved in dry DMSO in N_2 atmosphere. DCC (340 mg, 1.64 mmol) and DMAP (200 mg, 1.64 mmol) were added to the reaction mixture and stirred at room temperature for 24 h. The mixture was extracted with dichloromethane and water to remove unreacted C-dots. Then, the organic phase was collected and dried in a vacuum oven.

Preparation of Paper-Based Strips of C-dots-R6G and Metal-Ion Sensing Test. Cellulose-based filter paper (ADVANTEC no. 2) was cut into a circle with a diameter of 0.25 cm and immersed in an ethanol solution of **C-dots-R6G** (1 mg/mL). After 5 min, the filter paper was removed from the solution and air-dried. The paper-based strip containing **C-dots-R6G** was exposed to metal ions in aqueous solution. After 5 min, the paper-based strip was removed from the aqueous solution and air-dried at room temperature. The changes in the fluorescence of the strip were investigated with a digital camera (Canon EOS 450D) and fluorescence spectrometer. The color shades of the digital images were analyzed using Photoshop (Adobe) to separate shades of red, green, and blue colors to a single-channel grayscale. The ImageJ software (National Institute of Health, USA) was used to analyze the JPEG images and to obtain numerical single-color coordinate values, which could disinguish the color of interest without background color.

RESULTS AND DISCUSSION

C-dots were synthesized via the microwave-assisted pyrolysis process using acrylic acid and 1,2-ethylenediamine as the carbon source and surface passivation agent, respectively, which enabled us to obtain C-dots with the amino functional group

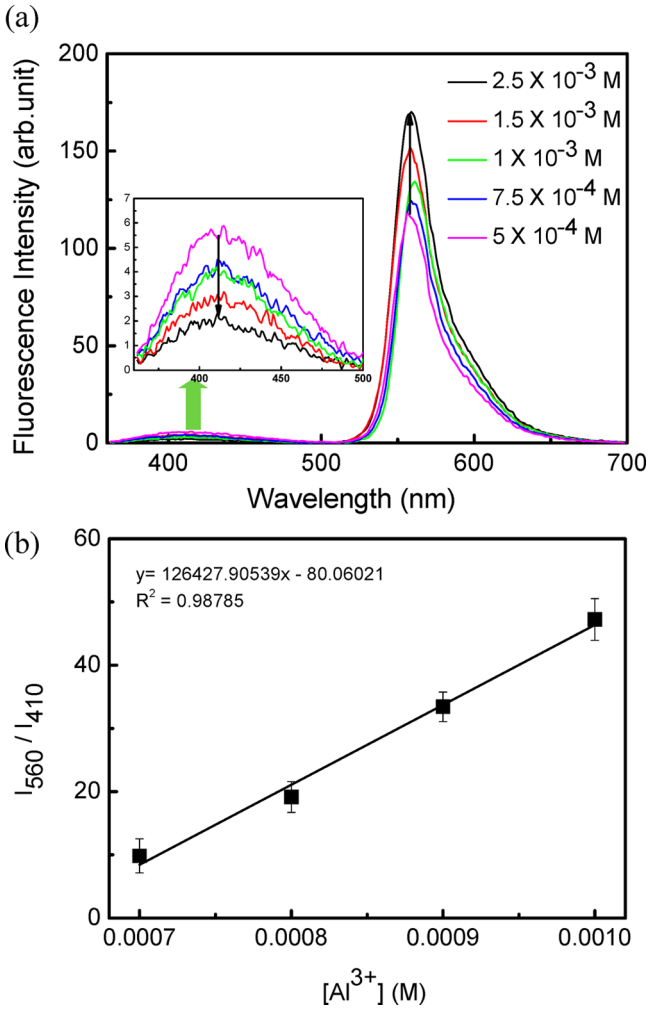

Figure 2. (a) Changes in emission spectra and (b) intensity ratios of **C-dots-R6G** at 560 and 410 nm upon exposure to Al^{3+} in ethanol solution. I_{560} and I_{410} correspond to the intensity of emission at 560 and 410 nm, respectively.

(Scheme S1).[57] The FT-IR spectrum showed that the C-dots had characteristic absorption bands of C−N at 1288 cm^{-1} and N−H at 3270 cm^{-1}, which indicated that the C-dots were successfully functionalized with the amine groups (Figure S1a). XPS revealed that the C-dots mainly consisted of C, O, and N elements, indicative of the presence of hydroxyl, amino, and carboxylic acid groups on the surface (Figure S1b). Moreover, the N 1s spectrum of the C-dots corresponded to the signals from the N−H group (399.63 eV). A typical TEM image of C-dots with a diameter of 5−20 nm can be observed in Figure S1c. The zeta potential of C-dots was determined to be +41.3 mV, mainly because of the presence of the amino groups on the surface of C-dots.

UV−vis absorption and fluorescence spectra of C-dots were investigated in aqueous solution (1 mg/mL) (Figure S2a). The absorption band was observed at 300 nm. The fluorescence spectra of the C-dots were highly dependent on the excitation wavelength (Figure S2b); therefore, any suitable excitation wavelength of C-dots could be employed to match a specific energy acceptor. The emission band position varied according to the different excitation wavelengths, primarily because of different emissive sites on the C-dots.[59−61] Upon excitation at 340 nm, the C-dots solution showed blue emission with the

DOI: 10.1021/acsami.5b04724
ACS Appl. Mater. Interfaces 2015, 7, 15649−15657

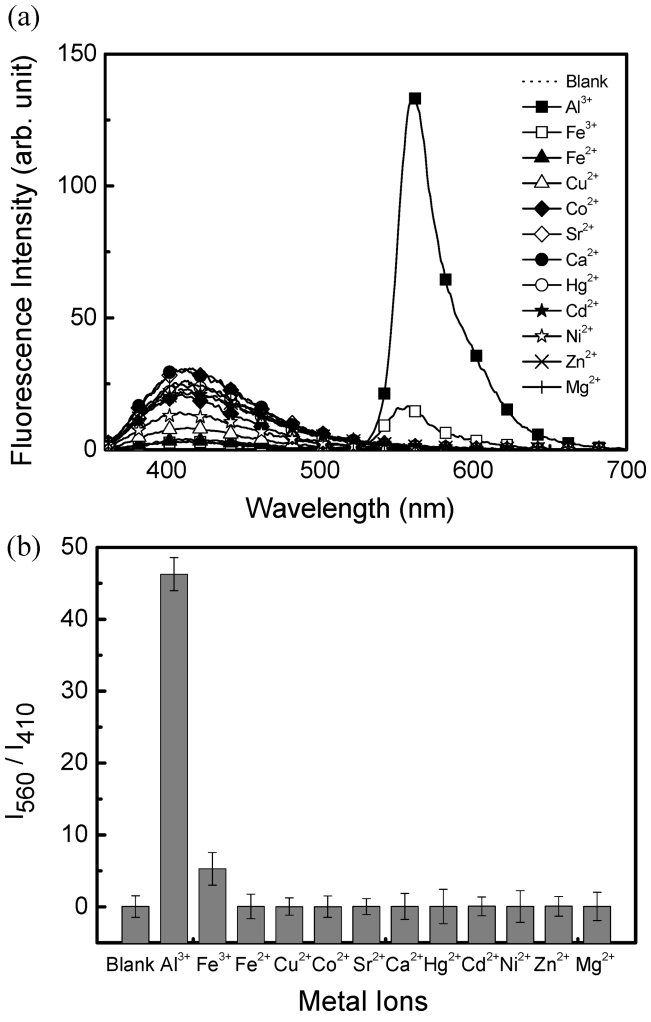

Figure 3. (a) Changes in fluorescence spectra and (b) intensity ratios of **C-dots-R6G** in response to various metal ions in ethanol. [metal ions] = 1×10^{-3} M.

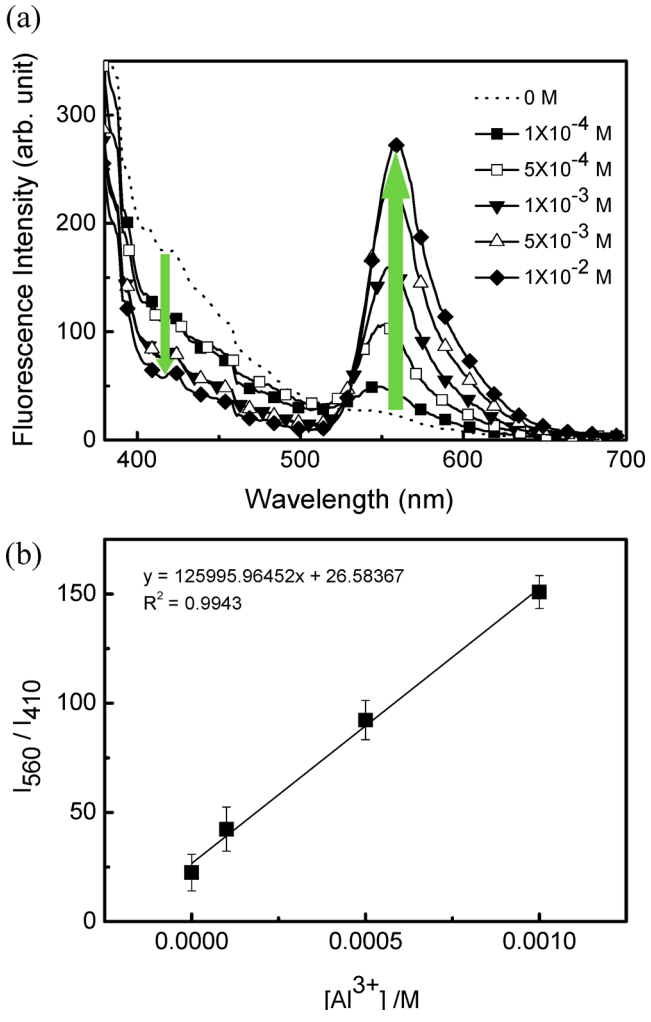

Figure 4. (a) Changes in emission intensity and (b) intensity ratios of the paper-based strips of **C-dots-R6G** at 560 and 410 nm upon exposure to Al^{3+} in aqueous solution. I_{560} and I_{410} correspond to the intensity of emission at 560 and 410 nm, respectively.

most intensified intensity around 410 nm, and the emission band was gradually red-shifted with excitation wavelength variation.

The FRET efficiency was strongly dependent on the following conditions: (1) The emission band of the donor should overlap with the absorption band of the acceptor. (2) The distance between both species should be in close proximity (less than 10 nm).[62] One of the advantages of C-dots as electron donor was that their emission wavelength can be manipulated by choosing different excitation wavelengths thus ensuring adaptability to any kinds of energy acceptors. For efficient FRET, the excitation wavelength of 350 nm was selected for excitation of C-dots (the energy donor) because the fluorescence at 350 nm excitation overlapped with the absorption band of R6G (the energy acceptor) to ensure the FRET process (Figure 1). Therefore, feasible energy transfer from C-dots to the rhodamine moiety was theoretically established.

R6G-COOH was synthesized in two steps using R6G as the starting material (Scheme S1). Intermediate **R6G-NH$_2$** was prepared in a reaction between R6G and 1,2-ethylenediamine according to the previous report.[58] **R6G-NH$_2$** was reacted with succinic acid to obtain **R6G-COOH**. The chemical structures of **R6G-NH$_2$** and **R6G-COOH** were confirmed by ^{1}H NMR and FT-IR. **R6G-COOH** was designed to become immobilized on the surface of C-dots through the reaction between the carboxylic acid group in **R6G-COOH** and the amino group in C-dots to form an amide linkage. Finally, rhodamine spirolactam was successfully incorporated in C-dots via the conventional DCC/DMAP method to obtain **C-dots-R6G** (Scheme 1).

FT-IR spectra revealed the changes in the functional groups on the surface of C-dots upon surface modification (Figure S3). The as-prepared C-dots showed the characteristic bands at 1630 cm^{-1} for C═C stretching, 2870 and 2940 cm^{-1} for C−H stretching, and a broad band at 3270 cm^{-1} corresponding to amine and hydroxyl groups. Upon surface modification with **R6G-COOH**, the characteristic absorption band of amide C═O stretching at 1670 cm^{-1} was observed, which indicated that the rhodamine moieties were successfully incorporated in the C-dots.

The amount of rhodamine moiety immobilized on the surface of C-dots was calculated from a calibration curve of rhodamine plotted with known concentrations of the open form of **R6G-COOH** at maximal absorption wavelength (λ_{max} = 526 nm) using UV spectroscopy (Figure S4). It was found that the rhodamine moiety was introduced on the surface of C-dots at 5.80×10^{-2} mg/mg. Moreover, the fluorescence intensity of **C-dots-R6G** under excitation at 350 nm (absorption of C-dots)

DOI: 10.1021/acsami.5b04724
ACS Appl. Mater. Interfaces 2015, 7, 15649−15657

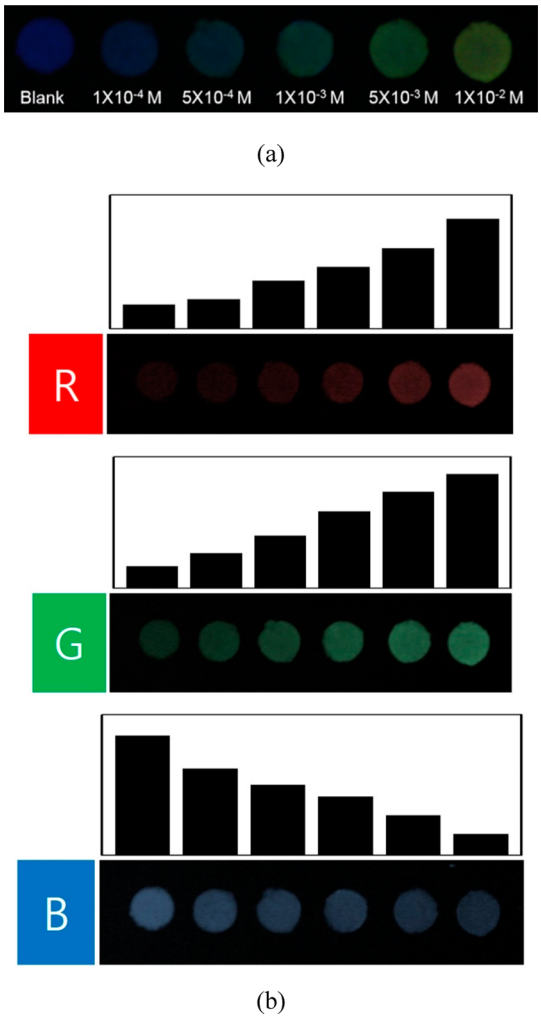

Figure 5. (a) Changes in the color of paper-based strips of **C-dots-R6G** in the presence of Al^{3+}. The photographic images represent the paper-based strips of **C-dots-R6G** under UV illumination (365 nm). (b) Intensities of red (R), green (G), and blue (B) channel images were obtained using Photoshop and ImageJ software to analyze the JPEG images. The heights of bars indicate the relative intensity of colors.

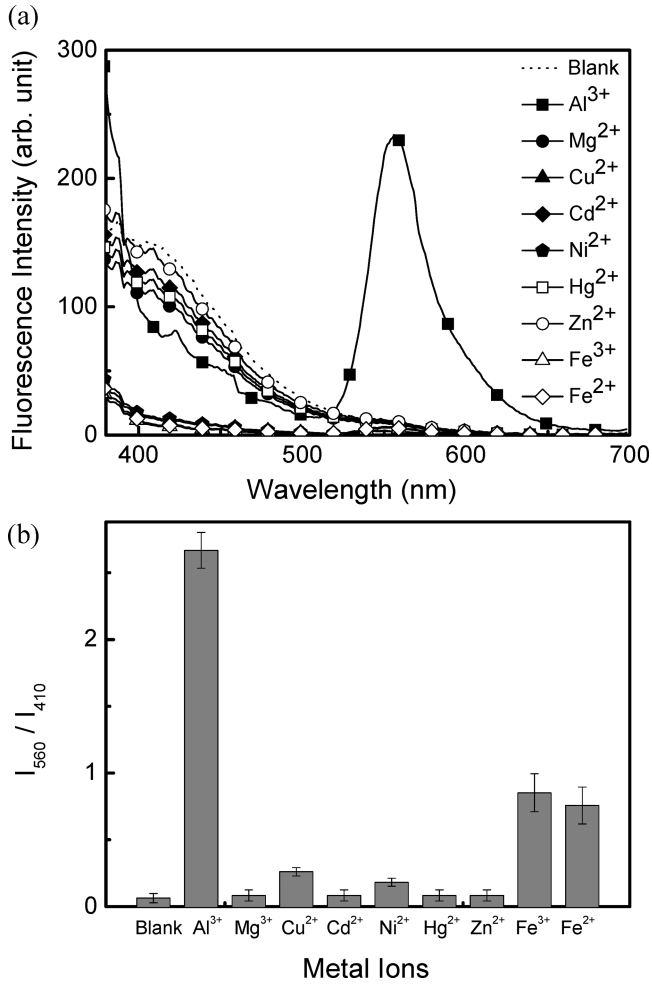

Figure 6. (a) Changes in fluorescence spectra and (b) ratios of fluorescence intensities (I_{560}/I_{410}) of paper-based strip of **C-dots-R6G** in response to various metal ions in aqueous solution. [metal ions] = 5×10^{-3} M.

was found to be more intensified than that under excitation at 526 nm (absorption of the open form of R6G), which demonstrated that the FRET process occurred spontaneously from the C-dots to the rhodamine moiety (Figure S4c).

The schematic illustration for the selective detection of Al^{3+} using **C-dots-R6G** is presented in Scheme 2. The C-dots serve as the energy donor as well as the conjugation site for the rhodamine moiety. The nanohybrid system showed only blue emission at 410 nm from C-dots because unopened rhodamine could not absorb the energy from C-dots' blue emission, leading to no FRET. Upon exposure to Al^{3+}, the spirolactam ring in the rhodamine moiety opened, and the absorption of the open form of rhodamine overlapped the emission of C-dots, in which the rhodamine moiety could serve as the energy acceptor, finally emitting yellow.

The addition of Al^{3+} to **C-dots-R6G** solution resulted in gradual decrease in the emission intensity at 410 nm with concomitant increase in the emission at 560 nm, exhibiting the blue-to-yellow emission color change. This could be clearly observed by the naked-eye under UV illumination (inset photos in Scheme 2). This phenomenon can be explained by the fact that the introduction of Al^{3+} induced dual changes in emissions, suggesting that the ratiometric detection of Al^{3+} was possible (Figure 2a). The limit of detection (LOD = $3\sigma/m$, where σ is the standard deviation of the blank measurements, and m is the slope of the intensity vs sample concentration) of **C-dots-R6G** in the solution for analysis of Al^{3+} was determined from the emission ratio of the two wavelengths (I_{560}/I_{410}) and was found to be 3.8×10^{-5} M (Figure 2b), which was comparable to previous reports.[63−66]

The selectivity of **C-dots-R6G** in ethanol solution for various metal ions was investigated by fluorescence measurements. The intensity ratio (I_{560}/I_{410}) was nearly unchanged in the presence of other metal ions (Figure 3). The addition of Al^{3+} contributed a considerable fluorescence enhancement at 560 nm because of FRET. This result indicated that **C-dots-R6G** exhibited specificity toward Al^{3+} over other metal ions. Evidence of the FRET process in the presence of Al^{3+} can be drawn from the data obtained using various excitation wavelengths (Figure S5). In the presence of Al^{3+}, the **C-dots-R6G** showed much enhanced emission intensity when excited at 350 nm (absorption of C-dots) rather than at 526 nm (absorption of the rhodamine moiety). In contrast, in the presence of Fe^{3+}, the emission excited at 526 nm was intensified compared to that at

DOI: 10.1021/acsami.5b04724
ACS Appl. Mater. Interfaces 2015, 7, 15649−15657

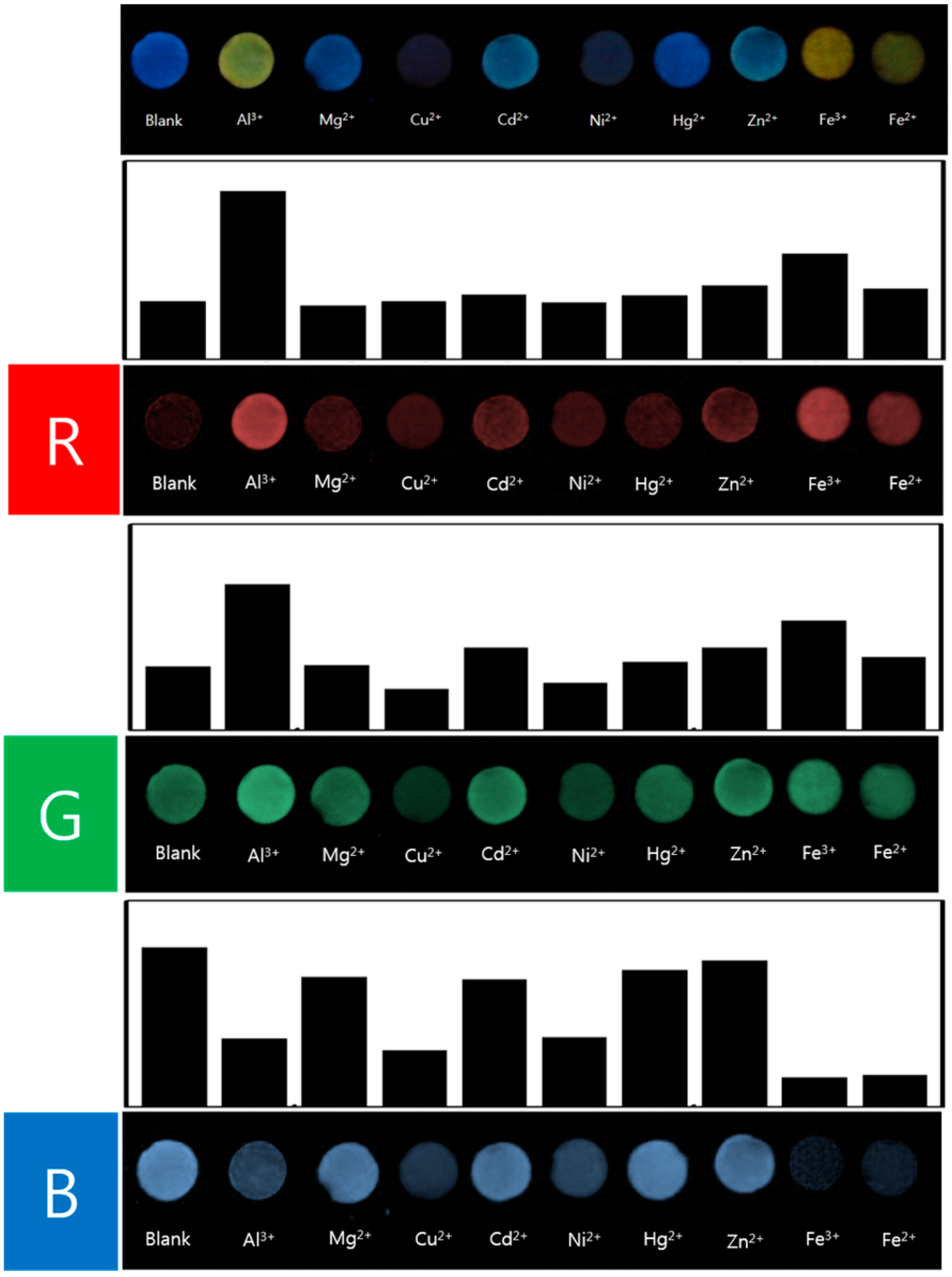

Figure 7. Changes in the color of paper-based strips of the paper-based strip of **C-dots-R6G** in the presence of various metal ions of 5×10^{-3} M in aqueous solutions. The photographic images represent the paper-based strips of **C-dots-R6G** under UV illumination (365 nm). Intensities of R, G, and B channel images were obtained using Photoshop and ImageJ software to analyze the JPEG images.

350 nm, indicating that the FRET occurred only in the presence of Al^{3+}.

Encouraged by the detection performance of **C-dots-R6G** in solution, we proceeded to investigate the detection potential of **C-dots-R6G** in the paper-based sensor strip. Cellulosic filter papers with immobilized **C-dots-R6G** were prepared by the immersion of the filter paper in ethanolic **C-dots-R6G** solution. We used filter papers as a sensing platform because of their interesting features, including the possibility of making a low-cost device, wide availability, ease of use and handling, and light weight, making them good media for analytical chemistry.[67]

The **C-dots-R6G**-containing paper-based strip was exposed to an aqueous solution of Al^{3+} for 5 min and then dried before the fluorescence measurement. The emission changes of the paper-based sensor strip upon exposure to different concentrations of Al^{3+} are shown in Figure 4a. Similar to the case of the detection in solution, as the concentration of Al^{3+} increased, the emission intensity of the sensor strip at 560 nm increased, whereas at 410 nm the intensity decreased. This result was attributed to the occurrence of FRET from the C-dots to the rhodamine moiety.

The relationship between the intensity ratios (I_{560}/I_{410}) and the concentration of Al^{3+} was determined quantitatively (Figure 4b). The fluorescence ratio showed a good linear relationship with the concentrations of Al^{3+} in the range of 1×10^{-4}–1×10^{-2} M, whose linearity (R = 0.9943) was better than that of detection in the solution (R = 0.988). The LOD from the paper-based strip showed a sensitivity of 3.89×10^{-5} M, similar to that of the solution, but had a range of detectable concentrations of Al^{3+} (0–1×10^{-3} M) broader than that of the solution.

DOI: 10.1021/acsami.5b04724
ACS Appl. Mater. Interfaces 2015, 7, 15649–15657

This indicated that the paper-based sensor was more effective and had better performance than the solution-based sensor.

Photographs of the paper-based strips containing **C-dots-R6G** were taken with a digital camera, and the images of color changes upon exposure to metal cations were analyzed using ImageJ software.[68,69] The color shades of the digital photographs were separated and converted into color values of red (R), green (G), and blue (B).[70] Figure 5a shows the changes in fluorescence color of the paper-based strip upon the addition of different concentrations of Al^{3+}. The changes in emission colors (blue to greenish-yellow) can be clearly observed as the concentration of Al^{3+} increases. To further elucidate that the changes in emission color resulted from FRET from C-dots to the rhodamine moiety, the emission colors were analyzed (Figure 5b). Upon exposure to Al^{3+}, the intensities of long-wavelength emissions (R and G from the energy acceptor) increased, whereas the intensity of short-wavelength emission (B from the energy donor) decreased because the lactam ring of the R6G moiety was open and thereby a spontaneous FRET process occurred from the C-dots to the rhodamine moiety.

To investigate the specificity of the paper-based strip of **C-dots-R6G** toward Al^{3+}, the fluorescence changes of the strip were studied in the presence of various metal ions. The sensor strip exhibited quite good selectivity for Al^{3+} with an emission color change to yellow, indicative of the high specificity of the paper-based sensor strip toward Al^{3+} over other metal ions (Figure 6). Results of color-intensity analysis of the paper-based strip in the presence of various metal ions including Al^{3+}, Mg^{2+}, Cu^{2+}, Co^{2+}, Ni^{2+}, Mg^{2+}, Zn^{2+}, Fe^{3+}, and Fe^{2+} are shown in Figure 7. The **C-dots-R6G**-based strip exhibited high selectivity toward Al^{3+} over other metal ions in terms of increased intensities in R and G and reduced intensity in B compared to the blank, indicative of the spontaneous energy transfer. The highly enhanced intensities in R and G of the strip toward Al^{3+} might be ascribed to the high specificity of the Al^{3+}-induced ring-opening reaction of the spirolactam structure of **C-dots-R6G** through chelation with the rhodamine moiety. The increase in the intensities of R and G and concomitant decrease in the intensity of B in the case of Fe^{3+} and Fe^{2+} resulted from the enhancement of yellow-emitting, ring-opened rhodamine moiety as well as quenching of the blue-emitting C-dots upon direct interaction with iron ions not from the FRET; this can also be found in previous results.[53]

In addition, competition experiments of the **C-dots-R6G** paper-based strip were performed in a mixture of other metal ions (Figure S6). Even in the mixture of metal ions, the sensor strip was responsive only to Al^{3+}, exhibiting intensified yellow fluorescence at 555 nm, indicating that the emission of the paper-based strip toward Al^{3+} was not affected by the presence of the other metal ions and demonstrating that our probe, **C-dots-R6G** paper-based strip, has potential applications in detecting Al^{3+} even in a contaminated solution that was mixed with other metal ions.

CONCLUSIONS

We have designed and synthesized rhodamine-appended C-dots to use as a FRET-based ratiometric probe for Al^{3+} in aqueous solution. The probe showed two well-resolved emission peaks of blue-emitting C-dots and yellow-emitting rhodamine moiety in the presence of Al^{3+}, which benefit FRET-based sensing (energy transfer from C-dots to the rhodamine moiety). In addition, such C-dots could be embedded to fabricate a paper-based sensor strip, in which the detection of Al^{3+} was performed in an aqueous solution. The paper-based sensor was based on the changes in the fluorescence response to Al^{3+} via the FRET process and resulted in high specificity to Al^{3+}, in which Al^{3+} induced the ring-opening of the rhodamine group. Such paper-based sensors provide a novel strategy for the design of selective probes for other targets with the potential advantages of easy handling, light weight, easy incorporation into devices, simplicity, cost effectiveness, and environmental friendliness. We expect that the probe offers a new approach for developing low-cost and selective sensors in diverse applications.

ASSOCIATED CONTENT

Supporting Information

UV and emission spectra of C-dots in aqueous solution; IR spectra, XPS spectra, and TEM image of C-dots; IR spectra of C-dots, **R6G-COOH**, and **C-dots-R6G**; calibration curve of **R6G-COOH**; and UV and fluorescence emission spectra, and metal-ion competition test of **C-dots-R6G**. The Supporting Information is available free of charge on the ACS Publications website at DOI: 10.1021/acsami.5b04724.

AUTHOR INFORMATION

Corresponding Author

*E-mail: tslee@cnu.ac.kr.

Notes

The authors declare no competing financial interest.

ACKNOWLEDGMENTS

Financial support from the National Research Foundation of Korea (NRF) funded by Korean government through the Basic Science Research Program (2015R1A2A2A05001134) is gratefully acknowledged.

REFERENCES

(1) Baker, S. N.; Baker, G. A. Luminescent Carbon Nanodots: Emergent Nanolights. *Angew. Chem., Int. Ed.* **2010**, *49*, 6726−6744.
(2) Li, H.; Kang, Z.; Liu, Y.; Lee, S.-T. Carbon nanodots: synthesis, properties and applications. *J. Mater. Chem.* **2012**, *22*, 24230−24253.
(3) Shen, J. H.; Zhu, Y. H.; Yang, X. L.; Li, C. Z. Graphene Quantum Dots: Emergent Nanolights for Bioimaging, Sensors, Catalysis and Photovoltaic Devices. *Chem. Commun.* **2012**, *48*, 3686−3699.
(4) Ray, S. C.; Saha, A.; Jana, N. R.; Sarkar, R. Fluorescent Carbon Nanoparticles: Synthesis, Characterization, and Bioimaging Application. *J. Phys. Chem. C* **2009**, *113*, 18546−18551.
(5) Tang, L. B.; Ji, R. B.; Cao, X. K.; Lin, J. Y.; Jiang, H. X.; Li, X. M.; Teng, K. S.; Luk, C. M.; Zeng, S. J.; Hao, J. H.; Lau, S. P. Deep Ultraviolet Photoluminescence of Water-Soluble Quantum Dots. *ACS Nano* **2012**, *6*, 5102−5110.
(6) Bourlinos, A. B.; Stassinopoulos, A.; Anglos, D.; Zboril, R.; Karakassides, M.; Giannelis, E. P. Surface Functionalized Carbogenic Quantum Dots. *Small* **2008**, *4*, 455−458.
(7) Xu, X. Y.; Ray, R.; Gu, Y. L.; Ploehn, H. J.; Gearheart, L.; Raker, K.; Scrivens, W. A. Electrophoretic Analysis and Purification of Fluorescent Single-Walled Carbon nanotube Fragments. *J. Am. Chem. Soc.* **2004**, *126*, 12736−12737.
(8) Liu, H. P.; Ye, T.; Mao, C. D. Fluorescent Carbon Nanoparticles Derived from Candle Soot. *Angew. Chem., Int. Ed.* **2007**, *46*, 6473−6475.
(9) Yang, Y.; Cui, J.; Zheng, M.; Hu, C.; Tan, S.; Xiao, Y.; Yang, Q.; Liu, Y. One-step Synthesis of Amino-functionalized Fluorescent Carbon Nanoparticles by Hydrothermal Carbonization of Chitosan. *Chem. Commun.* **2012**, *48*, 380−382.

DOI: 10.1021/acsami.5b04724
ACS Appl. Mater. Interfaces 2015, 7, 15649−15657

(10) Zhai, X.; Zhang, P.; Liu, C.; Bai, T.; Li, W.; Dai, L.; Liu, W. Highly Luminescent Carbon Nanodots by Microwave-assisted Pyrolysis. *Chem. Commun.* **2012**, *48*, 7955−7957.
(11) Cao, L.; Wang, X.; Meziani, M. J.; Lu, F. S.; Wang, H. F.; Luo, P. J. G.; Lin, Y.; Harruff, B. A.; Veca, L. M.; Murray, D.; Xie, S. Y.; Sun, Y. P. Carbon Dots for Multiphoton Bioimaging. *J. Am. Chem. Soc.* **2007**, *129*, 11318−11319.
(12) Gokus, T.; Nair, R. R.; Bonetti, A.; Böhmler, M.; Lombardo, A.; Novoselov, K. S.; Geim, A. K.; Ferrari, A. C.; Hartschuh, A. Making Graphene Luminescent by Oxygen Plasma Treatment. *ACS Nano* **2009**, *3*, 3963−3968.
(13) Xie, Z.; Wang, F.; Liu, C. Organic-Inorganic Hybrid Functional Carbon Dot Gel Glasses. *Adv. Mater.* **2012**, *24*, 1716−1721.
(14) Zheng, M.; Xie, Z.; Qu, D.; Li, D.; Du, P.; Jing, X.; Sun, Z. On-Off-On Fluorescent Carbon Dot Nanosensor for Recognition of Chromium (VI) and Ascorbic Acid Based on the Inner Filter Effect. *ACS Appl. Mater. Interfaces* **2013**, *5*, 13242−13247.
(15) Wang, J.; Wang, C.-F.; Chen, S. Amphiphilic Egg-Derived Carbon Dots: Rapid Plasma Fabrication, Pyrolysis Process, and Multicolor Pyrolysis Process, and Multicolor Printing Patterns. *Angew. Chem., Int. Ed.* **2012**, *51*, 9297−9301.
(16) Choi, Y.; Kim, S.; Choi, M.-H.; Ryoo, S.-R.; Park, J.; Min, D.-H.; Kim, B.-S. Highly Biocompatible Carbon Nanodots for Simultaneous Bioimaging and Targeted Photodynamic Therapy In Vitro and In Vivo. *Adv. Funct. Mater.* **2014**, *24*, 5781−5789.
(17) Li, W.; Zhang, Z.; Kong, B.; Feng, S.; Wang, J.; Wang, L.; Yang, J.; Zhang, F.; Wu, P.; Zhao, D. Simple and Green Synthesis of Nitrogen-Doped Photoluminescent Carbonaceous Nanospheres for Bioimaging. *Angew. Chem., Int. Ed.* **2013**, *52*, 8151−8155.
(18) Tao, H.; Yang, K.; Ma, Z.; Wan, J.; Zhang, Y.; Kang, Z.; Liu, Z. In Vivo NIR Fluorescence Imaging, Biodistribution, and Toxicology of Photoluminescent Carbon Dots Produced from Carbon Nanotubes and Graphite. *Small* **2012**, *8*, 281−290.
(19) Lai, C.-W.; Hsiao, Y.-H.; Peng, Y.-K.; Chou, R.-T. Facile Synthesis of Highly Emissive Carbon Dots from Pyrolysis of Glycerol; Gram Scale Production of Carbon Dots/mSiO_2 for Cell Imaging and Drug Release. *J. Mater. Chem.* **2012**, *22*, 14403−14409.
(20) Wang, Z. X.; Zheng, C. L.; Li, Q. L.; Ding, S. N. Electrochemiluminescence of a NanoAg-Carbon Nanodot Composite and Its Application to Detect Sulfide Ions. *Analyst* **2014**, *139*, 1751−1755.
(21) Shen, L.; Chen, M.; Hu, L.; Chen, X.; Wang, J. Growth and Stabilization of Silver Nanoparticles on Carbon Dots and Sensing Application. *Langmuir* **2013**, *29*, 16135−16140.
(22) Salinas-Castillo, A.; Ariza-Avidad, M.; Pritz, C.; Camprubí-Robles, M.; Fernández, B.; Ruedas-Rama, M. J.; Megia-Fernández, A.; Lapresta-Fernández, A.; Santoyo-Gonzalez, F.; Schrott-Fischer, A.; Capitan-Vallvey, L. F. Carbon Dots for Copper Detection with Down and Upconversion Fluorescent Properties as Excitation Sources. *Chem. Commun.* **2013**, *49*, 1103−1105.
(23) Chen, P. C.; Chen, Y. N.; Hsu, P. C.; Shih, C. C.; Chang, H. T. Photoluminescent Organosilane-Functionalized Carbon Dots as Temperature Probes. *Chem. Commun.* **2013**, *49*, 1639−1641.
(24) Zheng, M.; Liu, S.; Li, J.; Zhao, H.; Guan, X.; Hu, X.; Xie, Z.; Jing, X.; Sun, Z. Integrating Oxaliplatin with Highly Luminescent Carbon Dots: an Unprecedented Theranostic Agent for Personalized Medicine. *Adv. Mater.* **2014**, *26*, 3554−3560.
(25) Tang, J.; Kong, B.; Wu, K. H.; Xu, M.; Wang, Y.; Wang, Y.; Zhao, D.; Zheng, G. Carbon Nanodots Featuring Efficient FRET for Real-Time Monitoring of Drug Delivery and Two-Photon Imaging. *Adv. Mater.* **2013**, *25*, 6569−6574.
(26) Li, H.; He, X.; Kang, Z.; Huang, H.; Liu, Y.; Liu, J.; Lian, S.; Tsang, C. H.; Yang, X.; Lee, S. T. Water-Soluble Fluorescent Carbon Quantum Dots and Photocatalyst Design. *Angew. Chem., Int. Ed.* **2010**, *49*, 4430−4434.
(27) Tu, X.; Ma, Y.; Cao, Y.; Huang, J.; Zhang, M.; Zhang, Z. PEGylated Carbon Nanoparticles for Efficient In vitro Photothermal Cancer Therapy. *J. Mater. Chem. B* **2014**, *2*, 2184−2192.
(28) Bhunia, S. K.; Saha, A.; Maity, A. R.; Ray, S. C.; Jana, N. R. Carbon Nanoparticle-Based Fluorescent Bioimaging Probes. *Sci. Rep.* **2013**, *3*, 1473.
(29) Tetsuka, H.; Asahi, R.; Nagoya, A.; Okamoto, K.; Tajima, I.; Ohta, R.; Okamoto, A. Optically Tunable Amino-Functionalized Graphene Quantum Dots. *Adv. Mater.* **2012**, *24*, 5333−5338.
(30) Fan, J.; Hu, M.; Zhan, P.; Peng, X. Energy Transfer Cassettes Based on Organic Fluorophores: Construction and Applications in Ratiometric Sensing. *Chem. Soc. Rev.* **2013**, *42*, 29−43.
(31) Yang, Y.; Zhao, Q.; Feng, W.; Li, F. Y. Luminescent Chemodosimeters for Bioimaging. *Chem. Rev.* **2013**, *113*, 192−270.
(32) Kwak, C. K.; Kim, D. G.; Kim, T. H.; Lee, C.-S.; Lee, M.; Lee, T. S. Simultaneous and Dual Emissive Imaging by Micro-Contact Printing on the Surface of Electrostatically Assembled Water-Soluble Poly (p-phenylene) Using FRET. *Adv. Funct. Mater.* **2010**, *20*, 3847−3855.
(33) Noh, J.; Jang, G.; Kim, J.; Kim, D.; Lee, T. S. Functionalized, Fluorescent, Conjugated Polymer Nanospheres for Protein Targeting via Förster Resonance Energy Transfer. *J. Nanosci. Nanotechnol.* **2015**, *15*, 1756−1759.
(34) Zhang, X. L.; Xiao, Y.; Qian, X. H. A Ratiometric Fluorescent Probe Based on FRET for Imaging Hg^{2+} Ions in Living Cells. *Angew. Chem., Int. Ed.* **2008**, *47*, 8025−8029.
(35) Lee, M. H.; Kim, J. S.; et al. Metal Ion Induced FRET OFF-ON in Tren/Dansyl-Appended Rhodamine. *Org. Lett.* **2008**, *10*, 213−216.
(36) Cao, X.; Lin, W.; Ding, Y. Ratio-Au: FRET-based Fluorescent Probe for Ratiometric Determination of Gold Ions and Nanoparticles. *Chem. - Eur. J.* **2011**, *17*, 9066−9069.
(37) Kim, S. H.; Choi, H. S.; Kim, J.; Lee, S. J.; Quang, D. T.; Kim, J. S. Novel Optical/Electrochemical Selective 1,2,3-Triazole Ring-Appended Chemosensor for the Al^{3+} Ion. *Org. Lett.* **2010**, *12*, 560−563.
(38) Dujols, V.; Ford, F.; Czarnik, A. W. A Long-Wavelength Fluorescent Chemodosimeter Selective for Cu (II) Ion in Water. *J. Am. Chem. Soc.* **1997**, *119*, 7386−7387.
(39) Yang, Y. K.; Yook, K. J.; Tae, J. A Rhodamine-Based Fluorescent and Colorimetric Chemodosimeter for the Rapid Detection of Hg^{2+} Ions in Aqueous Media. *J. Am. Chem. Soc.* **2005**, *127*, 16760−16761.
(40) Wu, Y.-X.; Li, J.-B.; Liang, L.-H.; Lu, D.-Q.; Zhang, J.; Mao, G.-J.; Zhou, L.-Y.; Zhang, X.-B.; Tan, W.; Shen, G.-L.; Yu, R.-Q. A Rhodamine-Appended Water-Soluble Conjugated Polymer: an Efficient Ratiometric Fluorescence Sensing Platform for Intracellular Metal-Ion Probing. *Chem. Commun.* **2014**, *50*, 2040−2042.
(41) Armstrong, B.; Tremblay, C.; Baris, D.; Theriault, G. Lung Cancer Mortality and Polynuclear Aromatic Hydrocarbons: a Case-Cohort Study of Aluminium Production Workers in Arvida, Quebec, Canada. *Am. J. Epidemiol.* **1994**, *139*, 250−262.
(42) Darbre, P. D. Aluminium, Antiperspirants and Breast Cancer. *J. Inorg. Biochem.* **2005**, *99*, 1912−1919.
(43) Meng, Q.; Liu, H.; Sen, C.; Cao, C.; Ren, J. A Novel Molecular Probe Sensing Polynuclear Hydrolyzed Aluminum by Chelation-Enhanced Fluorescence. *Talanta* **2012**, *99*, 464−470.
(44) Kaur, K.; Bhardwaj, V. K.; Kaur, N.; Singh, N. Imine Linked Fluorescent Chemosensor for Al^{3+} and Resultant Complex as a Chemosensor for HSO_4^- Anion. *Inorg. Chem. Commun.* **2012**, *18*, 79−82.
(45) Gupta, V. K.; Singh, A. K.; Kumawat, L. K. Thiazole Schiff Base Turn-on Fluorescent Chemosensor for Al^{3+} Ion. *Sens. Actuators, B* **2014**, *195*, 98−108.
(46) Li, Y. P.; Liu, X. M.; Zhang, Y. H.; Chang, Z. A Fluorescent and Colorimetric Sensor for Al^{3+} Based on a dibenzo-18-crown-6 Derivative. *Inorg. Chem. Commun.* **2013**, *33*, 6−9.
(47) Cassella, R. J.; Magalhaes, O. I. B.; Couto, M. T.; Lima, E. L. S.; Neves, M. A. F. S.; Coutinho, F. M. B. Synthesis and Application of a Functionalized Resin for Flow Injection/F AAS Copper Determination in Waters. *Talanta* **2005**, *67*, 121−128.
(48) Mashhadizadeh, M. H.; Pesteh, M.; Talakesh, M.; Sheikhshoaie, I.; Ardakani, M. M.; Karimi, M. A. Solid Phase Extraction of Copper (II) by Sorption on Octadecyl Silica Membrane Disk Modified with a

DOI: 10.1021/acsami.5b04724
ACS Appl. Mater. Interfaces 2015, 7, 15649−15657

New Schiff Base and Determination with Atomic Absorption Spectrometry. *Spectrochim. Acta, Part B* **2008**, *63*, 885−888.
(49) Goyal, R. N.; Gupta, V. K.; Chatterjee, S. Electrochemical Oxidation of 2′, 3′-Dideoxyadenosine at Pyrolytic Graphite Electrode. *Electrochim. Acta* **2008**, *53*, 5354−5360.
(50) Goyal, R. N.; Gupta, V. K.; Chatterjee, S. Simultaneous Determination of Adenosineand Inosine Using Single-Wall Carbon Nanotubes Modified Pyrolytic Graphite Electrode. *Talanta* **2008**, *76*, 662−668.
(51) Jain, R.; Gupta, V. K.; Jadon, N.; Radhapyari, K. Voltammetric Determination of Cefixime in Pharmaceuticals and Biological Fluids. *Anal. Biochem.* **2010**, *407*, 79−88.
(52) Yu, C.; Li, X.; Zeng, F.; Zheng, F.; Wu, S. Carbon-dot-based Ratiometric Fluorescent Sensor for Detecting Hydrogen Sulfide in Aqueous Media and Inside Live Cells. *Chem. Commun.* **2013**, *49*, 403−405.
(53) Lan, M.; Zhang, J.; Chui, Y.-S.; Wang, P.; Chen, X.; Lee, C.-S.; Kwong, H.-L.; Zhang, W. Carbon Nanoparticle-based Ratiometric Fluorescent Sensor for Detecting Mercury Ions in Aqueous Media and Living Cells. *ACS Appl. Mater. Interfaces* **2014**, *6*, 21270−21278.
(54) Su, S.; Ali, M. M.; Filipe, C. D. M.; Li, Y.; Pelton, R. Microgel-based Inks for Paper-Supported Biosensing Applications. *Biomacromolecules* **2008**, *9*, 935−941.
(55) Guo, Z.; Zhu, W.; Zhu, M.; Wu, X.; Tian, H. Near-Infrared Cell-Permeable Hg^{2+} -Selective Ratiometric Fluorescent Chemodosimeters and Fast Indicator Paper for $MeHg^{+}$ Based on Tricarbocyanines. *Chem. - Eur. J.* **2010**, *16*, 14424−14432.
(56) Jo, S.; Kim, D.; Son, S.-H.; Kim, Y.; Lee, T. S. Conjugated Poly(fluorine-quinoxaline) for Fluorescence Imaging and Chemical Detection of Nerve Agents with Its Paper-Based Strip. *ACS Appl. Mater. Interfaces* **2014**, *6*, 1330−1336.
(57) Zhang, P.; Li, W.; Zhai, X.; Liu, C.; Dai, L.; Liu, W. A Facile and Versatile Approach to Biocompatible "Fluorescent Polymers" from Polymerizable Carbon Nanodots. *Chem. Commun.* **2012**, *48*, 10431−10433.
(58) Wang, Y.; Wu, H.; Luo, J.; Liu, X. Synthesis of an Amphiphilic Copolymer Bearing Rhodamine Moieties and Its Self-assembly into Micelles as Chemosensors for Fe^{3+} in Aqueous Solution Reactive & Functional. *React. Funct. Polym.* **2012**, *72*, 169−175.
(59) Ding, Z. F.; Quinn, B. M.; Haram, S. K.; Pell, L. E.; Korgel, B. A.; Bard, A. J. Electrochemistry and Electrogenerated Chemiluminescence from Silicon Nanocrystal Quantum Dots. *Science* **2002**, *296*, 1293−1297.
(60) Zhou, J. G.; Booker, C.; Li, R. Y.; Zhou, X. T.; Sham, T. K.; Sun, X. L.; Ding, Z. F. An Electrochemical Avenue to Blue Luminescent Nanocrystals from Multiwalled Carbon Nanotubes (MWCNTs). *J. Am. Chem. Soc.* **2007**, *129*, 744−745.
(61) Bao, L.; Zhang, Z.-L.; Tian, Z.-Q.; Zhang, L.; Liu, C.; Lin, Y.; Qi, B.; Pang, D.-W. Electrochemical Tuning of Luminescent Carbon Nanodots: from Preparation to Luminescence Mechanism. *Adv. Mater.* **2011**, *23*, 5801−5806.
(62) Morawetz, H. Studies of Synthetic Polymers by Nonradiative Energy Transfer. *Science* **1988**, *240*, 172−176.
(63) Gupta, V. K.; Shoora, S. K.; Kumawat, L. K.; Jain, A. K. A Highly Selective Colorimetric and Turn-on Fluorescent Chemosensor based on 1-(2-pyridylazo)-2-naphthol for the Detection of Aluminium (III) Ions Sens. *Sens. Actuators, B* **2015**, *209*, 15−24.
(64) Fan, L.; Li, T. R.; Wang, B. D.; Yang, Z. Y.; Liu, C. J. A Colorimetric and Turn-on Fluorescent Chemosensor for Al (III) based on a Chromone Schiff-base Spectrochim. *Spectrochim. Acta, Part A* **2014**, *118*, 760−764.
(65) Iniya, M.; Jeyanthi, D.; Krishnaveni, K.; Chellappa, D. A Bifunctional Chromogenic and Fluorogenic Probe for F^{-} and Al^{3+} based on Azo-benzimidazole Conjugate. *J. Lumin.* **2015**, *157*, 383−389.
(66) Dong, M.; Dong, Y. M.; Ma, T. H.; Wang, Y. W.; Peng, Y. A Highly Selective Fluorescence-enhanced Chemosensor for Al^{3+} in Aqueous Solution based on a Hybrid Ligand from BINOL Scaffold and β-amino Alcohol. *Inorg. Chim. Acta* **2012**, *381*, 137−142.
(67) Eaidkong, T.; Mungkarndee, R.; Phollookin, C.; Tumcharern, G.; Sukwattanasinitt, M.; Wacharasindhu, S. Polydiacetylene Paper-based Colorimetric Sensor Array for Vapor Phase Detection and Identification of Volatile Organic Compounds. *J. Mater. Chem.* **2012**, *22*, 5970−5977.
(68) Schindelin, J.; Arganda-Carreras, I.; Frise, E.; Kaynig, V.; Longair, M.; Pietzsch, T.; Preibisch, S.; Rueden, C.; Saalfeld, S.; Schmid, B.; Tinevez, J. Y.; White, D. J.; Hartenstein, V.; Eliceiri, K.; Tomancak, P.; Cardona, A. Fiji: an Open-source Platform for Biological-image Analysis. *Nat. Methods* **2012**, *9*, 676−682.
(69) Song, Y.; Wang, Z.; Li, L.; Shi, W.; Li, X.; Ma, H. Gold Nanoparticles Functionalized with Cresyl Violet and and Porphyrin via Hyaluronic Acid for Targeted Cell Imaging and Phototherapy. *Chem. Commun.* **2014**, *50*, 15696−15698.
(70) Matkowskyj, K. A.; Schonfeld, D.; Benya, R. V. Quantitative Immunohistochemistry by Measuring Culmulative Signal Strength Using Commercially Available Software Photoshop and Matlab. *J. Histochem. Cytochem.* **2000**, *48*, 303−311.

DOI: 10.1021/acsami.5b04724
ACS Appl. Mater. Interfaces 2015, 7, 15649−15657